

Metal–Organic Frameworks

Three Series of Sulfo-Functionalized Mixed-Linker CAU-10 Analogues: Sorption Properties, Proton Conductivity, and Catalytic Activity

Nele Reimer,^[a] Bart Bueken,^[b] Sebastian Leubner,^[a] Christopher Seidler,^[c] Michael Wark,^[c] Dirk De Vos,^[b] and Norbert Stock^{*[a]}

Abstract: Ten mixed-linker metal–organic frameworks [Al(OH)(*m*-BDC-*X*)_{1–*y*}(*m*-BDC-SO₃H)_{*y*}] (H₂BDC = 1,3-benzenedicarboxylic acid; X = H, NO₂, OH) exhibiting the CAU-10-type structure were synthesized. The compounds can be grouped into three series according to the combination of ligands employed. The three series of compounds were obtained by employing different ratios of *m*-H₂BDC-*X* and *m*-H₂BDC-SO₃Li. The resulting compounds, which are denoted CAU-10-H/*Sx*, -N/*Sx* and -O/*Sx*, show exceptionally high thermal stability for sulfonated materials of up to 350 °C. Detailed characterization with special focus on polarity and acidity was performed, and the impact of the additional SO₃H groups is

clearly demonstrated by changes in the sorption affinities/capacities towards several gases and water vapor. In addition, selected samples were evaluated for proton conductivity and as catalysts for the gas-phase dehydration of ethanol to ethylene. While only very low proton conductivities were observed, a pronounced increase in catalytic activity was achieved. Although reactions were performed at temperatures of 250 and 300 °C for more than 40 h, no desulfonation and no loss of crystallinity were observed, and stable ethanol conversion resulted. This demonstrates the high stability of this material.

Introduction

Metal–organic frameworks (MOFs) have attracted much attention in the last few years due to their potential applications in the fields of gas storage and separation, drug delivery, and catalysis.^[1] MOFs are built up from inorganic building units, for example, metal ions or clusters, which are interconnected by organic linker molecules, forming, in general, three-dimensional porous structures. This modular assembly allows for tuning of properties by chemical functionalization of the organic part or by replacement of the inorganic unit. This approach is called isorecticular chemistry^[2] and has previously been applied to several well-known framework structures.^[3] Recently, another concept to design compounds with desired properties has been established. In the so-called mixed-linker approach, differently

functionalized linker molecules are incorporated in one framework to selectively influence the characteristics of a compound.^[4]

For example, Al-MIL-53, [Al(OH)(BDC-*X*)], is a flexible compound based on (functionalized) 1,4-benzenedicarboxylic acid [H₂BDC-*X*] and chains of *trans* corner-sharing AlO₆ octahedra.^[3a,5] Its flexibility and thermal stability strongly depend on the nature of the functionalized linker molecule. By using a mixture of H₂BDC and H₂BDC-NH₂ it was possible to influence these properties by means of the ratio of the incorporated linker molecules.^[6] In another recent study, mixed-linker MOFs based on the CAU-10, [Al(OH)(*m*-BDC-*X*)], structure were synthesized to fine-tune the sorption properties of this compound.^[7] CAU-10 is built up from helical chains of *cis* corner-sharing AlO₆ octahedra interconnected by isophthalate ions. A series of isorecticular compounds has been synthesized with several functionalized isophthalic acids. Depending on the functional group of the linker molecule, the structure of each derivative is slightly altered. This results in different uptake capacities, affinities, and accessibilities of the pores of each compound towards different adsorbates.^[3c]

The incorporation of sulfonic acid groups in MOFs is of great interest. Due to their strongly acidic protons, compounds bearing these groups show potential for catalytic or proton conduction applications.^[8] The sorption properties of such compounds can also be influenced. Recently, it was reported that the introduction of sulfo groups in the zirconium-based compound UiO-66 led to a strong increase in the sorption selectivity.

[a] N. Reimer, S. Leubner, Prof. N. Stock
Institut für Anorganische Chemie
Christian-Albrechts-Universität zu Kiel
Max-Eyth-Strasse 2, 24118 Kiel (Germany)
E-mail: stock@ac.uni-kiel.de

[b] B. Bueken, Prof. D. De Vos
Centre for Surface Chemistry and Catalysis
University of Leuven
Kasteelpark Arenberg 23, 3001 Leuven (Belgium)

[c] C. Seidler, Prof. M. Wark
Institut für Chemie, Carl von Ossietzky Universität Oldenburg
Carl-von-Ossietzky-Strasse 9–11, 26129 Oldenburg (Germany)

Supporting information for this article is available on the WWW under <http://dx.doi.org/10.1002/chem.201501502>.

ty for CO₂ over CH₄ compared to the unfunctionalized compound.^[9] The synthesis of SO₃H-functionalized MOFs is not always easily accomplished. Only a few examples are known in which the acid group was directly introduced into the framework by the use of a monosodium sulfoterephthalate organic linker molecule.^[8a,10] Another way to introduce sulfo groups is through post-synthetic modification, which was demonstrated by Chen et al. using Cr-MIL-101, Zr-UiO-66, and Al-MIL-53.^[8c,11]

We focused our research on aluminum-based MOFs, because these compounds are known for their high thermal and chemical stability.^[3a,c,12] In addition, the starting materials are inexpensive and of low toxicity, which makes them interesting for industrial usage.^[13] The goal of the present study was to combine the properties of Al-MOFs and sulfo-functionalized compounds. Therefore, we chose CAU-10 as the parent structure and employed isorecticular synthesis using 5-sulfo isophthalic acid monolithium salt (*m*-H₂BDC-SO₃Li). Pure *m*-H₂BDC-SO₃Li as the organic linker does not lead to the CAU-10 analogue; hence, mixtures of linkers were used. By adopting the synthesis conditions of the already known compounds CAU-10-H, -NO₂, and -OH, we were able to synthesize three series of mixed-linker compounds with the CAU-10 structure with different fractions of sulfonic acids incorporated into the framework: [Al(OH)(*m*-BDC-H)_{1-y}(*m*-BDC-SO₃H)_y]-solvent ($y=0.08, 0.15, 0.205, 0.24$; CAU-10-H/S1 to CAU-10-H/S4); [Al(OH)(*m*-BDC-NO₂)_{1-y}(*m*-BDC-SO₃H)_y]-solvent ($y=0.065, 0.10, 0.175, 0.215$; CAU-10-N/S1 to CAU-10-N/S4) and [Al(OH)(*m*-BDC-OH)_{1-y}(*m*-BDC-SO₃H)_y]-solvent ($y=0.08, 0.125$; CAU-10-O/S1 and CAU-10-O/S2); for further details see Experimental Section]. The obtained compounds were characterized by IR and NMR spectroscopy, thermal and elemental analysis, powder XRD (PXRD), and sorption measurements. Selected samples were investigated with regard to their proton conductivity and catalytic performance in the dehydration of ethanol.

Results and Discussion

PXRD investigations and crystal structure

The structure of the CAU-10 framework is built up from helical chains of *cis* corner-sharing AlO₆ polyhedra.^[3c] The three-dimensionality of the framework results from the connection of each helix to four adjacent helices with alternating rotational orientation through the carboxylate groups of (functionalized) isophthalate ions (Figure 1). Square-shaped channels with a maximum diameter of about 7 Å are formed. The pores can be modulated by the use of functionalized linker molecules^[3c] or in a mixed-linker approach by the use of differently functionalized linker molecules.^[7]

All mixed-linker compounds in this study were obtained as microcrystalline powders. The SEM image of CAU-10-H/S1 is shown in Figure 2 (SEM images of CAU-10-H/S2–4 are shown in Figures S1–S3 of the Supporting Information). For example, the PXRD patterns of the CAU-10-H/S_x samples are compared to that of CAU-10-H in Figure 3. The mixed-linker compounds are also highly crystalline. Compared to the PXRD pattern of CAU-10-H, only changes in the relative intensities of the reflec-

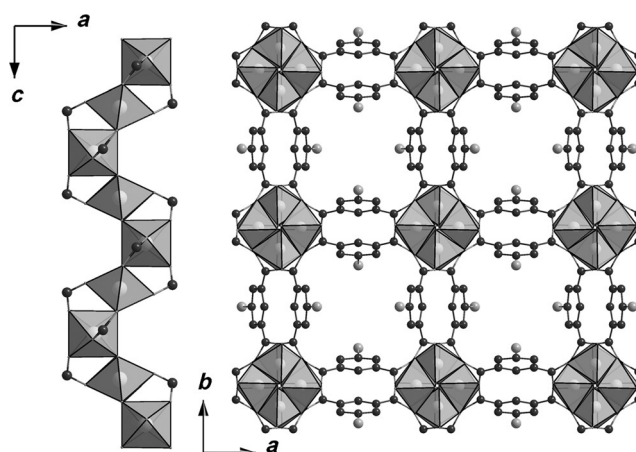


Figure 1. Structure of CAU-10. Al atoms are displayed in very light gray, O atoms in gray, and C atoms in dark grey. The light gray atoms represent possible functional groups.

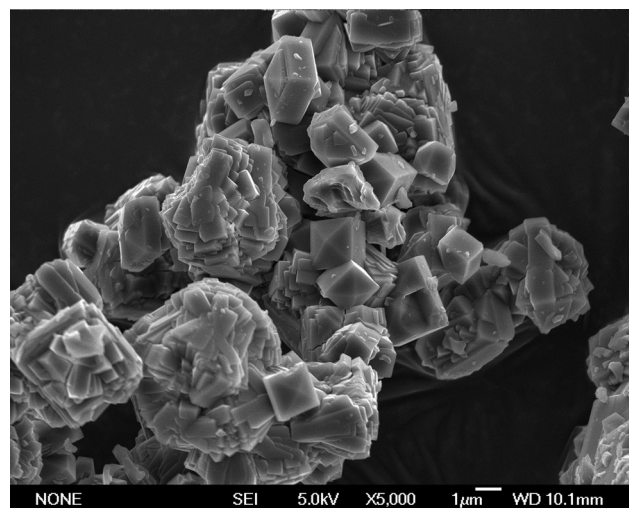


Figure 2. SEM image of CAU-10-H/S1.

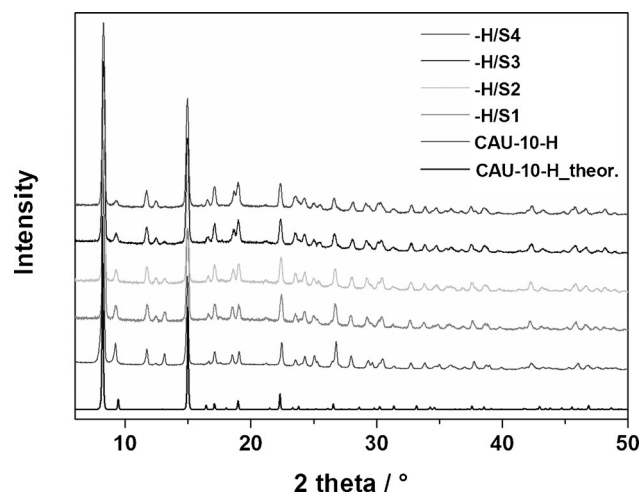


Figure 3. PXRD measurements for the mixed-linker compounds CAU-10-H/S_x compared to the theoretical and experimental patterns of CAU-10-H.

tions up to 20° (2θ) are observed, which become more pronounced with increasing amounts of SO_3H groups. This can be explained by the additional electron density within the pores due to the incorporated sulfo groups.

The PXRD patterns of CAU-10-N/Sx and CAU-10-O/Sx are compared with those of CAU-10- NO_2 and CAU-10-OH in Figure S4 of the Supporting Information. The mixed-linker compounds are obtained in high crystallinity, and the positions and relative intensities of all reflections are in good accordance with those of CAU-10- NO_2 and CAU-10-OH. The high-resolution PXRD patterns of all compounds were indexed by using TOPAS Academics.^[14] The resulting cell parameters were refined by using the Pawley method,^[14] and only slight changes compared to those of the parent structures were observed (Table 1). The Pawley fits are shown in Figures S5–S14 of the Supporting Information.

Table 1. Results of the Pawley refinements.				
Sample CAU-10-	Space group	$a=b$ [Å]	c [Å]	R_{wp} [%]
H	$I4_1$	21.55(7)	10.38(3)	1.9
H/S1	$I4_1$	21.3846(6)	10.7424(5)	5.7
H/S2	$I4_1$	21.4262(8)	10.6918(6)	5.2
H/S3	$I4_1$	21.4786(6)	10.6635(5)	4.4
H/S4	$I4_1$	21.4896(5)	10.6277(5)	4.8
NO_2	$P4_1$	21.4707(3)	10.3777(2)	3.2
N/S1	$P4_1$	21.532(1)	10.409(1)	4.0
N/S2	$P4_1$	21.539(1)	10.421(1)	3.3
N/S3	$P4_1$	21.525(1)	10.416(1)	3.6
N/S4	$P4_1$	21.514(2)	10.405(2)	3.2
OH	$P4$	21.3072(5)	38.6974(9)	4.8
O/S1	$P4$	21.325(1)	38.793(2)	4.2
O/S2	$P4$	21.285(2)	38.792(5)	5.5

Vibrational spectroscopy

IR spectra of all compounds were collected after washing the samples with water. For example, the spectra of CAU-10-H/Sx, $m\text{-H}_2\text{BDC-SO}_3\text{Li}$, and CAU-10-H are shown in Figure 4. The box marks the characteristic vibrations of the SO_3H groups and it is clearly visible that, with increasing amount of SO_3H groups, the intensities of the characteristic bands increase.

There are no indications for uncoordinated linker molecules, since no bands around 1700 cm^{-1} due to free carboxyl groups are observed. The characteristic stretching modes of the carboxylate groups of the mixed-linker compounds are in accordance with those of the single linker compound. The presence of sulfo groups is verified by the vibrations between 1250 and 1000 cm^{-1} (black box). The asymmetric and symmetric vibrations of the sulfo groups are observed at $\tilde{\nu}_{\text{O}=\text{S}=\text{O}}=1223$ and 1160 cm^{-1} , respectively, and at $\tilde{\nu}_{\text{S}-\text{O}}=1044\text{ cm}^{-1}$. The in-plane skeletal vibration of the sulfonic acid substituted benzene ring appears at $\tilde{\nu}=1080\text{ cm}^{-1}$ and the C–S vibration at $\tilde{\nu}=629\text{ cm}^{-1}$. The C–H out-of-plane vibrations for the 1,3-substituted benzene rings, which are observed at $\tilde{\nu}=725$ and 755 cm^{-1} , are marked with stars. For the 1,3,5-substituted benzene ring this vibration appears at $\tilde{\nu}=782\text{ cm}^{-1}$ and is marked with a plus sign.^[8b,15] The IR spectra of CAU-10-N/Sx and CAU-

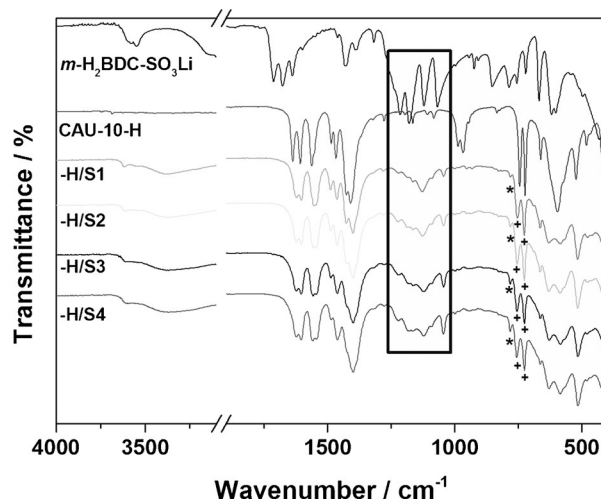


Figure 4. IR spectra of CAU-10-H/Sx compared to those of CAU-10-H and $m\text{-H}_2\text{BDC-SO}_3\text{Li}$. The star marks the out-of-plane CH vibration of the 1,3,5-substituted linker molecules and the plus sign the same vibration for the 1,3-substituted linker. The box marks the area of the SO_3H vibrations.

10-O/Sx are compared to those of the linker molecule and the respective single-linker compound in Figures S15 and S16 of the Supporting Information. Again, no unconsumed linker molecules are observed in the spectra, and the characteristic vibrations for the sulfo groups are present.

Thermal Analysis

To investigate the thermal stability, thermogravimetric (TG) measurements of all compounds were performed under air. The results for the CAU-10-H/Sx samples are shown in Figure 5. All TG curves exhibit a two-step weight loss. The first step up to around 300°C can be attributed to the removal of incorporated H_2O and DMF molecules. Around 400°C the frameworks start to decompose, and X-ray amorphous Al_2O_3 is formed at temperatures above 600°C . The TG measurements of the CAU-10-N/Sx and -O/Sx samples are shown in Figures S17 and S18

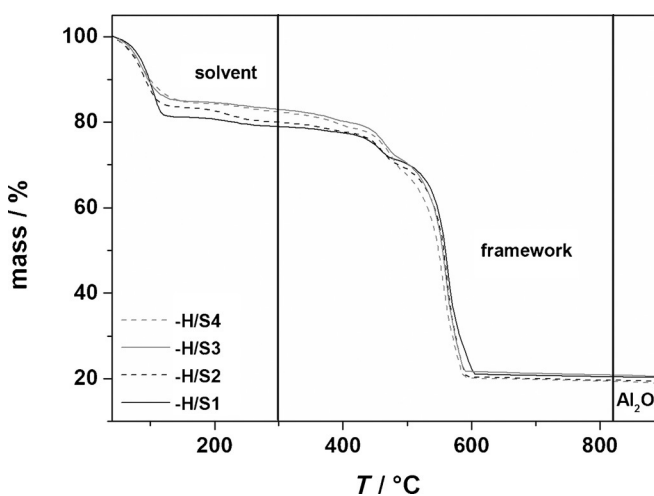


Figure 5. TG measurements of the CAU-10-H/Sx samples.

of the Supporting Information. Again, two-step weight losses were observed. The removal of incorporated solvent molecules is completed at about 250 °C for CAU-10-N/Sx and about 230 °C for CAU-10-O/Sx. Above these temperatures the frameworks slowly start to decompose into X-ray amorphous Al₂O₃.

Sorption properties

To investigate the influence of the incorporated sulfo groups in the different functionalized CAU-10 analogues, sorption measurements with different adsorptives were performed. N₂ and H₂ (up to 1 bar) measurements were carried out at 77 K and CO₂ (up to 1 bar), and H₂O vapor measurements at 298 K.

For CAU-10-H/Sx it was only possible to record a N₂ isotherm for the compound with the lowest degree of doping due to very long equilibration times (Supporting Information, Figure S19). The pore volume is decreased to 0.21 cm³g⁻¹ and the specific surface area to 372 m²g⁻¹ compared to CAU-10-H ($V_{\text{mic}}=0.25$ cm³g⁻¹, $a_s=635$ m²g⁻¹). All CAU-10-N/Sx samples show a type I isotherm characteristic of microporous materials (Supporting Information, Figure S20). The specific surface area decreases with increasing amount of sulfo groups incorporated into the framework. The single-linker compound CAU-10-OH does not adsorb any nitrogen. However, for the mixed linker compounds a small uptake is observed (Supporting Information, Figure S21). The incorporation of sulfo groups perhaps leads to a more ordered orientation of the linker molecules due to interactions of the functional groups, so that the pores become accessible for nitrogen molecules.

Water-vapor sorption measurements for all mixed-linker compounds are compared to those of the single-linker parents in Figure 6. According to Canivet et al., three parameters should be considered to characterize the samples concerning their hydrophobicity/hydrophilicity.^[16] The capacity c reflects the accessible pore volume, indicator $\alpha=p/p_0$ gives the relative pressure at which 50% of the capacity is reached, and the slope of the isotherm at low relative pressures is relevant to describing the affinity.

In all cases, with increasing amount of incorporated SO₃H groups the α parameter shifts to lower p/p_0 values and the slope at low relative pressures increases, which indicates increasing affinity towards water vapor and therefore higher hydrophilicity. For CAU-10-H/Sx the capacity decrease is clearly due to the additional space required by the SO₃H groups. For CAU-10-N/Sx only small changes in the sorption capacity are observed, since the replacement of a NO₂ group by an SO₃H group probably only slightly affects the pore volume. The same can be assumed for the CAU-10-O/Sx samples. The strong affinity towards water vapor suggests potential application of these materials in the field of humidity sensing, and therefore they are currently under investigation. For the CO₂ measurements the same trend was observed. In all cases the affinity increases with increasing amount of incorporated SO₃H groups (Supporting Information, Figures S22–S24). The capacities of CAU-10-H/Sx (Supporting Information, Figure S27) and -N/Sx (Supporting Information, Figure S23) decrease but, interestingly, that of CAU-10-O/Sx (Supporting Information, Fig-

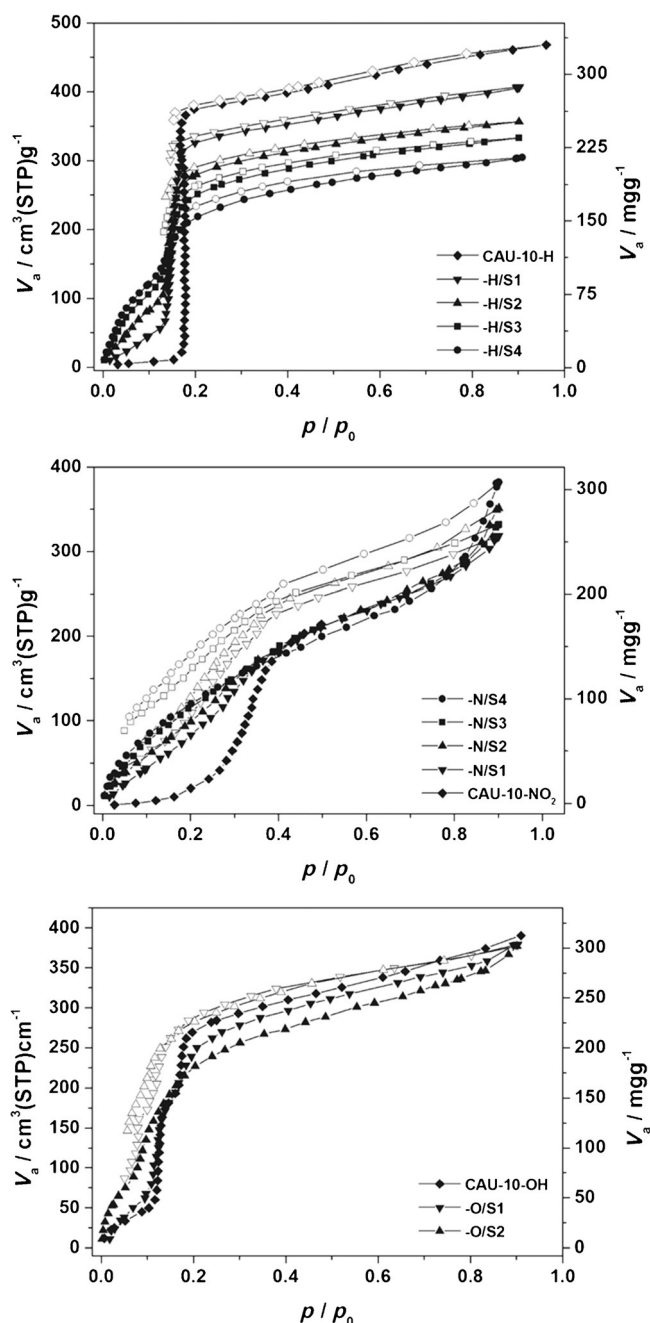


Figure 6. Water-vapor sorption isotherms of the mixed-linker compounds compared to those of the single-linker counterparts. Top: CAU-10-H/Sx. Middle: CAU-10-N/Sx. Bottom: CAU-10-O/Sx.

ure S24) increases. Apparently, the presence of OH and SO₃H groups leads to strong interactions between the linker molecules, which could lead to a polarizing effect of the pore surface that strongly affects the affinity. This behavior has previously been observed for the mixed-linker compound CAU-10-NO₂/NH₂.^[7]

Since hydrogen is a small nonpolar molecule, the polarity of the introduced sulfo groups does not affect the affinity towards this gas, and only the reduced pore volume influences the sorption behavior of the materials. Therefore, for all materials a reduced sorption capacity for H₂ is observed, but no

Table 2. Results of the sorption measurements.

Sample CAU-10-	N ₂ (77 K) a_s [m ² g ⁻¹]/ V_{mic} [cm ³ g ⁻¹]	H ₂ (77 K) [wt%]	CO ₂ (298 K) [wt%]	H ₂ O (298 K) [cm ³ g ⁻¹]
H	635/0.25	1.12	10.57	468
H/S1	372/0.21	1.03	10.52	407
H/S2	–	0.95	9.88	357
H/S3	–	0.91	9.44	329
H/S4	–	0.85	8.87	305
NO ₂	440/0.18	1.01	8.71	215 ^[a]
N/S1	324/0.15	0.91	8.61	318
N/S2	270/0.13	0.81	8.29	351
N/S3	242/0.12	0.69	7.72	332
N/S4	158/0.09	0.64	7.12	382
OH	–	0.79	5.57	390
O/S1	67/0.04	0.77	6.57	379
O/S2	74/0.05	0.69	8.04	377

[a] $p/p_0 = 0.5$

change in their affinity (Supporting Information, Figures S25–S27). Trend graphs comparing the affinities and capacities of all compounds towards H₂O vapor and CO₂ gas as well as the specific surface areas are shown in Figures S28–S30 of the Supporting Information; Table 2 summarizes the results of the sorption measurements of all compounds.

Proton conductivity

Due to the presence of SO₃H groups the proton conductivity of selected compounds, that is, CAU-10-H/S1, CAU-10-N/S2, and CAU-10-O/S2 were determined. Previous conductivity measurements on Al-MIL-53-OSO₃H (degree of sulfation of Al-MIL-53: 50%) showed high proton conductivities at temperatures up to 333 K, which were on the same order of magnitude as observed for Nafion.^[17] The samples in our study contain smaller amounts of SO₃H groups, but roughly the same fraction. All investigated CAU-10 samples exhibited low proton conductivity (Supporting Information, Figure S31). Only for CAU-10-O/S2 was it possible to determine proton conductivities in the whole temperature range. The obtained values were between 2.74×10^{-7} and 8.61×10^{-6} S cm⁻¹. For CAU-10-N/S2, conductivities ranging from 1.71×10^{-8} to 5.61×10^{-7} S cm⁻¹ were found in the temperature range of 373–413 K. A proton conductivity of 4.88×10^{-7} S cm⁻¹ at 413 K was determined for CAU-10-H/S1. Since the amount of SO₃H groups is similar in all three samples, the roles of the H, NO₂, and OH groups determine the proton conductivity. In combination with hydroxyl groups higher proton conductivities could be determined over the whole temperature range. Observed values are one order of magnitude higher, which could be due to the fact that both functional groups can be protonated and deprotonated and thus participate in the proton-conducting mechanism. In contrast, the amount of SO₃H groups in CAU-10-H/S1 and CAU-10-N/S2 does not lead to a sufficient density of functional groups for a constant proton-conduction pathway. Only with increasing temperature, and therefore increasing mobility of the functional groups and the protons, can proton conductivity occur.

Catalytic experiments

The combination of well-defined pore spaces, the presence of strongly acidic SO₃H groups and high thermal stabilities make the mixed-linker CAU-10 MOFs potentially interesting catalysts. Selected samples were evaluated as catalysts for the gas-phase dehydration of ethanol to ethylene (Table 3).

Table 3. Ethanol dehydration over mixed-linker CAU-10 samples.^[a]

Sample CAU-10-	X_{EtOH} [%]	$S_{C_2=}$ [%]	$S_{C_2O_2}$ [%]	$S_{C_2=O}$ [%]
H ^[b]	7	22	70	8
H/S2 ^[b]	27	22	76	2
H/S4 ^[b]	52	27	71	2
N/S4 ^[b]	15	30	69	1
H ^[c]	56	52	42	6
H/S4 ^[c]	91	79	20	1

[a] X_{EtOH} = ethanol conversion, $S_{C_2=}$ = ethylene selectivity, $S_{C_2O_2}$ = diethyl ether selectivity, $S_{C_2=O}$ = acetaldehyde selectivity. [b] 250 °C; feed rate 6.9 mmol mmol_{MOF}⁻¹ h⁻¹; 300 mg catalyst. [c] 300 °C.

The presence of SO₃H groups in the mixed-linker CAU-10 materials clearly results in a strong increase in catalyst activity. The parent CAU-10-H shows only a very modest ethanol conversion of 7% at 250 °C, mainly due to the presence of weakly acidic μ_2 -OH groups decorating the inorganic chains, a situation similar to those in MIL-53(Al) and the aluminum fumarate A520.^[18] Under identical reaction conditions, however, CAU-10-H/S2 and CAU-10-H/S4 achieved ethanol conversions of 27 and 52%, respectively, which indicate that in these materials the more acidic protons of the SO₃H groups dominate as the Brønsted acidic active sites. Furthermore, a higher degree of *m*-H₂BDC-SO₃H doping correlates with a higher activity. However, CAU-10-N/S4 only reaches a conversion of 15% (250 °C), in spite of its high SO₃H content. It is likely that the relatively bulky NO₂ groups restrict diffusion through the one-dimensional pore system and thus result in lower conversions. When the reaction temperature is increased to 300 °C, the reactivity differences between CAU-10-H and CAU-10-H/S4 become more pronounced, with ethanol conversions of 56 and 91%, respectively.

For this reaction to proceed selectively towards the olefin product, elevated reaction temperatures and relatively strong acidic sites are required.^[19] Although at 250 °C the ethylene selectivity between CAU-10-H and the SO₃H-bearing materials does not differ strongly, this picture changes drastically at 300 °C, at which CAU-10-H/S4 achieves an ethylene selectivity of 79%. In stark contrast, CAU-10-H only achieves a selectivity to ethylene of 52%. Notably, both at 250 °C and 300 °C, a significant amount of acetaldehyde is formed over CAU-10-H. This dehydrogenation product is typically associated with the presence of basic sites. For instance, the carboxylate groups of isophthalic acid could act as proton acceptor sites. For the mixed-linker compounds, acetaldehyde is formed in far lower yield, which indicates that mainly the Brønsted acidic SO₃H sites lining the pore interior participate in the dehydration reaction.

Furthermore, only trace amounts of oligomerization products were observed (butenes < 0.2%). However, for CAU-10-N/S4 reaction at 300 °C, even for short reaction times, led to strong browning of the material and appearance of compounds of higher molecular weight in the gas chromatogram, which indicate that this material promotes undesired condensation and oligomerization side reactions.

The stability of the mixed-linker CAU-10 samples under the applied reaction conditions was confirmed by powder XRD and the observation of stable conversion and selectivity profiles with extended reaction times, as is illustrated for CAU-10-H/S4 in Figure 7 and for CAU-10-H in Figure S32 of the Supporting Information. This was further confirmed by the lack of desulfonation (Supporting Information, Figure S33) of the used catalysts. The high thermal stability of the CAU-10-H/Sx materials is in stark contrast to many organic SO₃H-containing resins, which typically suffer from desulfonation starting at 150 °C.^[20]

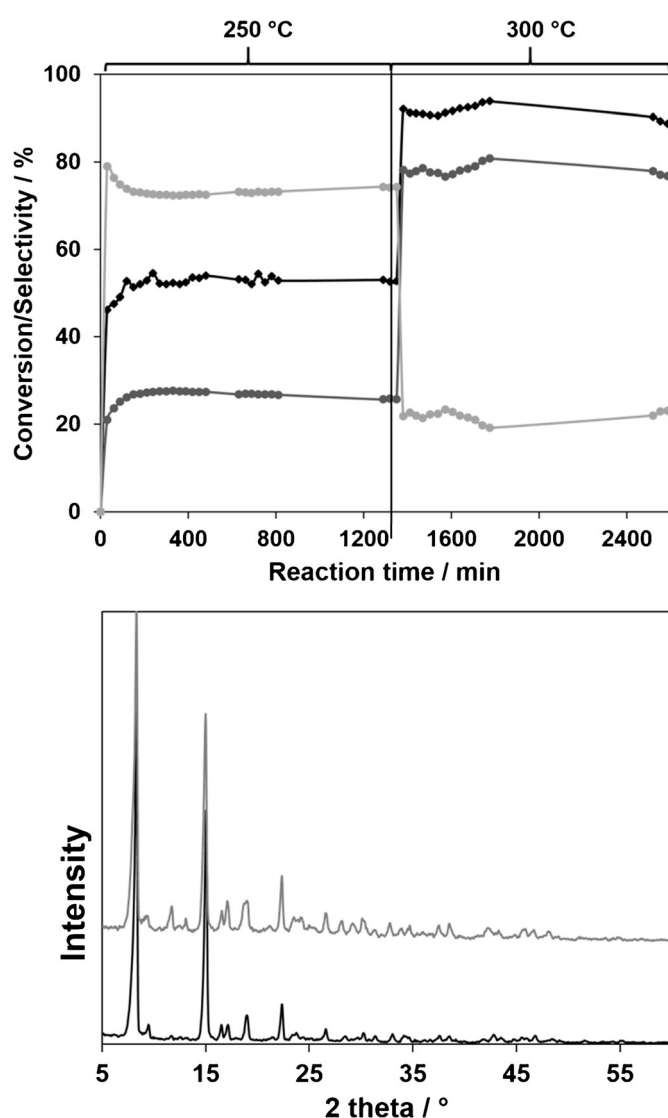


Figure 7. Top: Ethanol conversion (black) and selectivities to ethylene (gray) and diethyl ether (light gray) over CAU-10-H/S4 (feed rate: 6.9 mmol g_{MOR}⁻¹ h⁻¹). Bottom: PXR pattern of CAU-10-H/S4 before (black) and after reaction (light gray).

Thus, the mixed-linker MOFs could serve as attractive alternatives to these resins in more demanding applications such as catalysis at elevated temperatures.

Conclusion

We have presented the synthesis of ten mixed-linker materials exhibiting the CAU-10 structure. The known compounds CAU-10-H, -NO₂, and -OH were chosen and the mixed-linker approach was used to introduce SO₃H groups in different fractions up to a maximum amount of 24% for CAU-10-H/S4. The SO₃H groups do not affect the high thermal stability of the materials, but the polarity of these groups strongly influences the sorption properties. Changes in sorption capacities and affinities towards several gases (N₂, H₂, CO₂) were observed, and a strong increase in affinity towards water vapor reveals a potential application in the field of humidity sensing, which is currently under investigation. Due to the strong acidity of the SO₃H groups, selected samples were evaluated for their proton conductivity and as catalysts for the gas-phase dehydration of ethanol to ethylene. Whereas only low proton conductivity was observed, the presence of SO₃H groups clearly results in a strong increase in catalytic activity. Although reactions were performed at 300 °C, stable conversion of ethanol, no loss in crystallinity, and no desulfonation were observed. This high thermal stability is in contrast to many SO₃H-containing resins, so these compounds could be an alternative candidate for catalysis at elevated temperatures. In comparison to many other MOFs, the CAU-10 compounds also exhibit exceptional stability towards water. The materials neither showed any loss of crystallinity during the water sorption experiments nor under the severe conditions of the proton conductivity measurements (up to 140 °C under 100% R.H.) and the catalytic reactions (dehydration of ethanol at 300 °C).

Experimental Section

Materials and methods

All chemicals are commercially available and were used without further purification. For the synthesis, custom-made steel autoclaves with Teflon inlets and a volume of 30 mL or glass reactors with a volume of 100 mL for solvothermal reaction conditions were used. The initial characterization by means of PXR methods was carried out on a STOE-Stadi-P Kombi diffractometer (Cu_{Kα1} radiation) equipped with an xy stage and an image-plate detector. The data for the indexing and Pawley refinements were collected on a STOE-Stadi-P diffractometer (Cu_{Kα1} radiation) equipped with a Mythen detector. The software used for Pawley refinements was TOPAS Academics v4.1.^[14] IR spectra were recorded on a Bruker ALPHA-FT-IR A220/D-01 spectrometer equipped with an ATR unit. The TG analyses were carried out with a NETZSCH STA 409 CD analyzer. The samples were heated in Al₂O₃ crucibles at a rate of 4 °C min⁻¹ under a flow of air (25 mL min⁻¹). The contents of carbon, hydrogen, nitrogen, and sulfur were determined by elemental chemical analysis on a EuroVector EuroEA Elemental Analyzer. Atomic absorption spectroscopy (AAS) for analysis of lithium was carried out using a PerkinElmer AAnalyst 300 spectrometer. Gas sorption experiments were performed with a BEL JAPAN INC.

Table 4. Linker ratios used in the synthesis and for the final compounds with the resulting molecular formulas for all compounds.

Sample	Ratio used in synthesis		Ratio calcd by ¹ H NMR		Molecular formula calcd by ¹ H NMR and TG analysis
CAU-10-H/S1	<i>m</i> -H ₂ BDC-H	<i>m</i> -H ₂ BDC-SO ₃ Li	<i>m</i> -BDC-H	<i>m</i> -BDC-SO ₃ H	[Al(OH)(<i>m</i> -BDC-H) _{0.92} (<i>m</i> -BDC-SO ₃ H) _{0.08}] _{3.5} ·3.5 H ₂ O·0.1 DMF
H/S2	0.825	0.125	0.92	0.08	[Al(OH)(<i>m</i> -BDC-H) _{0.85} (<i>m</i> -BDC-SO ₃ H) _{0.15}] _{2.5} ·2.5 H ₂ O·0.1 DMF
H/S3	0.75	0.25	0.85	0.15	[Al(OH)(<i>m</i> -BDC-H) _{0.795} (<i>m</i> -BDC-SO ₃ H) _{0.205}] ₂ ·2 H ₂ O·0.2 DMF
H/S4	0.625	0.375	0.795	0.205	[Al(OH)(<i>m</i> -BDC-H) _{0.76} (<i>m</i> -BDC-SO ₃ H) _{0.24}] _{1.5} ·1.5 H ₂ O·0.2 DMF
CAU-10-N/S1	<i>m</i> -H ₂ BDC-NO ₂	<i>m</i> -H ₂ BDC-SO ₃ Li	<i>m</i> -BDC-NO ₂	<i>m</i> -BDC-SO ₃ H	[Al(OH)(<i>m</i> -BDC-NO ₂) _{0.935} (<i>m</i> -BDC-SO ₃ H) _{0.065}] _{2.23} ·2.23 H ₂ O
N/S2	0.825	0.125	0.935	0.065	[Al(OH)(<i>m</i> -BDC-NO ₂) _{0.85} (<i>m</i> -BDC-SO ₃ H) _{0.15}] ₃ ·3.08 H ₂ O
N/S3	0.75	0.25	0.90	0.10	[Al(OH)(<i>m</i> -BDC-NO ₂) _{0.825} (<i>m</i> -BDC-SO ₃ H) _{0.175}] _{2.97} ·2.97 H ₂ O
N/S4	0.625	0.375	0.825	0.175	[Al(OH)(<i>m</i> -BDC-NO ₂) _{0.785} (<i>m</i> -BDC-SO ₃ H) _{0.215}] _{2.93} ·2.93 H ₂ O
CAU-10-O/S1	<i>m</i> -H ₂ BDC-OH	<i>m</i> -H ₂ BDC-SO ₃ Li	<i>m</i> -BDC-OH	<i>m</i> -BDC-SO ₃ H	[Al(OH)(<i>m</i> -BDC-OH) _{0.92} (<i>m</i> -BDC-SO ₃ H) _{0.08}] _{4.7} ·4.7 H ₂ O
O/S2	0.825	0.125	0.92	0.08	[Al(OH)(<i>m</i> -BDC-NO ₂) _{0.875} (<i>m</i> -BDC-SO ₃ H) _{0.125}] _{4.68} ·4.68 H ₂ O

Belsorp_{max} instrument. Measurements with N₂ and H₂ were performed at -196 °C, and measurements with CO₂ and H₂O vapor at 25 °C. Prior to each measurement all samples were activated at 200 °C overnight at 10⁻² kPa. Solution-state ¹H NMR spectroscopy was performed on a Bruker DRX500/Bruker Advance 200 spectrometer. Prior to the measurements 2–3 mg of each sample was dissolved in a mixture of NaOD (5%) and D₂O (95%). SEM images of gold-sputtered samples were collected on a Philips XL30 FEG microscope. Catalytic investigations were performed on an in-house-constructed continuous flow reactor (Supporting Information, Figure S34). For each MOF, the reactor was loaded with a sample containing adsorbed atmospheric water, which was removed prior to reaction by outgassing the sample overnight at 150 °C under an N₂ flow (5 mL min⁻¹). In each case, the resulting amount of dry material was 300 mg. An N₂ flow (10 mL min⁻¹) was saturated with ethanol by passing it through a bubbler containing pure ethanol (Fischer), which was kept thermostatically at 40 °C. This N₂ flow was allowed to equilibrate with ethanol for 4 h prior to reaction. The resulting gas mixture was passed over the catalyst bed (feed rate: 6.9 mmol g_{MOF}⁻¹ h⁻¹) at different reaction temperatures (250, 275, and 300 °C). By using a gas-sample loop, samples were collected at 30 min intervals (5 s sampling time) and analyzed with an on-line gas chromatograph (GC Shimadzu 2010 plus chromatograph with FID detector, GsBP-1 column; 100 m, 250 μm inner diameter). Data handling was performed with the GCsolution Analysis software (v 2.3). The proton conductivity was determined by electrochemical impedance spectroscopy^[21] in a two-electrode cell setup with a Zahner Zennium workstation. Measurements were carried out between 1 Hz and 1 MHz (100 mV) at temperatures ranging from 333–413 K at 100% relative humidity (R.H.).^[22] Further details are presented in the Supporting Information.

Synthesis

The exact amounts of starting materials for the synthesis of all compounds are listed in Table S1 of the Supporting Information. According to the synthesis conditions of CAU-10-H,^[3c] the syntheses of the CAU-10-H/Sx samples were carried out in custom-made steel autoclaves with Teflon inlets and a volume of 30 mL. In a typical procedure for CAU-10-H/S1, a mixture of a 1 M aqueous solution of Al₂(SO₄)₃·18H₂O (920 μL, 1.38 mmol), *m*-H₂BDC (200.6 mg, 1.21 mmol), *m*-H₂BDC-SO₃Li (43.5 mg, 0.172 mmol), 1.15 mL of DMF, and 3.68 mL of H₂O was placed in one of these vessels and the reaction was performed in an oven at 135 °C for 12 h with 1 h heating and cooling ramp. The resulting precipitate was filtered off, intensively washed with water, and dried in air at room tem-

perature. The syntheses of the CAU-10-N/Sx and the CAU-10-O/Sx samples were carried out in 100 mL glass reactors equipped with a screw cap. In a typical procedure for CAU-10-N/S1, a mixture of a 2 M aqueous solution of AlCl₃·6H₂O (3400 μL, 6.8 mmol), *m*-H₂BDC-NO₂ (1260 mg, 5.97 mmol), *m*-H₂BDC-SO₃Li (214.9 mg, 0.853 mmol), 4.0 mL of DMF, and 12.6 mL of H₂O was placed in one of the vessels. In a typical procedure for CAU-10-O/S1, a mixture of a 2 M aqueous solution of AlCl₃·6H₂O (2800 μL, 5.6 mmol), *m*-H₂BDC-OH (874.9 mg, 4.80 mmol), *m*-H₂BDC-SO₃Li (173.3 mg, 0.686 mmol), 4.0 mL of DMF, and 13.2 mL of H₂O were used. In both cases the reaction was performed in an oven at 120 °C for 12 h with 2 h heating and cooling ramps. The resulting precipitate was filtered off, intensively washed with water, and dried in air at room temperature. IR spectroscopy showed no residues of uncoordinated linker molecules. To determine the fraction of the incorporated linker molecules and thus to assign the molecular formula, solution ¹H NMR measurements were performed (Supporting Information, Figure S35–37) on digested samples. On the basis of the integral ratios of the protons of the different linker molecules, the actual ratios were calculated (Table 4). The results of the elemental analysis agree well with the compositions of all compounds determined from thermogravimetric (TG) and ¹H NMR measurements (Supporting Information, Table S2). The acidic character of the samples was verified by a simple indicator test. On addition of H₂O/methyl red a color change from yellow to pink was observed, indicating an acidic pH value (Supporting Information, Figure S38). The exchange of the Li⁺ ions against H⁺ ions at the SO₃H groups was verified by AAS.

Acknowledgements

We acknowledge Dr. Helge Reinsch (CAU Kiel) for fruitful discussions. This work has been supported by the DFG (SPP 1362, WA 1116/17-2 and STO 643/5-2). B.B. and D.D.V. gratefully acknowledge the Research Foundation Flanders (FWO) for financial support (Aspirant grant).

Keywords: aluminum · conducting materials · heterogeneous catalysis · metal–organic frameworks · microporous materials

- [1] a) Themed issue on Metal-Organic Frameworks, *Chem. Soc. Rev.* **2009**, *38*, 1201–1508; b) Themed issue on Metal-Organic Frameworks, *Chem. Soc. Rev.* **2012**, *41*, 673–1268; c) Themed issue on Metal-Organic Frameworks, *Chem. Soc. Rev.* **2014**, *43*, 5415–6172.

- [2] O. M. Yaghi, M. O'Keeffe, N. W. Ockwig, H. K. Chae, M. Eddaoudi, J. Kim, *Nature* **2003**, 423, 705–714.
- [3] a) S. Biswas, T. Ahnfeldt, N. Stock, *Inorg. Chem.* **2011**, 50, 9518–9526; b) M. Lammert, S. Bernt, F. Vermoortele, D. E. De Vos, N. Stock, *Inorg. Chem.* **2013**, 52, 8521–8528; c) H. Reinsch, M. A. van der Veen, B. Gil, B. Marszalek, T. Verbiest, D. de Vos, N. Stock, *Chem. Mater.* **2013**, 25, 17–26; d) H. Deng, S. Grunder, K. E. Cordova, C. Valente, H. Furukawa, M. Hmadeh, F. Gándara, A. C. Whalley, Z. Liu, S. Asahina, H. Kazumori, M. O'Keeffe, O. Terasaki, J. F. Stoddart, O. M. Yaghi, *Science* **2012**, 336, 1018–1023; e) P. Horcajada, H. Chevreau, D. Heurtaux, F. Benyettou, F. Salles, T. Devic, A. Garcia-Marquez, C. Yu, H. Lavrard, C. L. Dutton, E. Magnier, G. Maurin, E. Elkaim, C. Serre, *Chem. Commun.* **2014**, 50, 6872–6874; f) M. Eddaoudi, J. Kim, N. Rosi, D. Vodak, J. Wachter, M. O'Keeffe, O. M. Yaghi, *Science* **2002**, 295, 469–472; g) S. J. Garibay, S. M. Cohen, *Chem. Commun.* **2010**, 46, 7700–7702.
- [4] a) A. D. Burrows, *CrystEngComm* **2011**, 13, 3623–3642; b) W. Lu, Z. Wei, Z.-Y. Gu, T.-F. Liu, J. Park, J. Park, J. Tian, M. Zhang, Q. Zhang, T. Gentle III, M. Bosch, H.-C. Zhou, *Chem. Soc. Rev.* **2014**, 43, 5561–5593; c) X. Kong, H. Deng, F. Yan, J. Kim, J. A. Swisher, B. Smit, O. M. Yaghi, J. A. Reimer, *Science* **2013**, 341, 882–885.
- [5] T. Loiseau, C. Serre, C. Huguénard, G. Fink, F. Taulelle, M. Henry, T. Bataille, G. Férey, *Chem. Eur. J.* **2004**, 10, 1373–1382.
- [6] a) S. Marx, W. Kleist, J. Huang, M. Maciejewski, A. Baiker, *Dalton Trans.* **2010**, 39, 3795–3798; b) T. Lescouet, E. Kockrick, G. Bergeret, M. Peratitus, D. Farrusseng, *Dalton Trans.* **2011**, 40, 11359–11361; c) T. Lescouet, E. Kockrick, G. Bergeret, M. Peratitus, S. Aguado, D. Farrusseng, *J. Mater. Chem.* **2012**, 22, 10287–10293.
- [7] H. Reinsch, S. Waitschat, N. Stock, *Dalton Trans.* **2013**, 42, 4840–4847.
- [8] a) G. Akiyama, R. Matsuda, H. Sato, M. Takata, S. Kitagawa, *Adv. Mater.* **2011**, 23, 3294–3297; b) Y. Zang, J. Shi, F. Zhang, Y. Zhong, W. Zhu, *Catal. Sci. Technol.* **2013**, 3, 2044–2049; c) J. Chen, K. Li, L. Chen, R. Liu, X. Huang, D. Ye, *Green Chem.* **2014**, 16, 2490–2499; d) P. Ramaswamy, R. Matsuda, W. Kosaka, G. Akiyama, H. J. Jeon, S. Kitagawa, *Chem. Commun.* **2014**, 50, 1144–1146; e) Z. Li, G. He, Y. Zhao, Y. Cao, H. Wu, Y. Li, Z. Jiang, *J. Power Sources* **2014**, 262, 372–379.
- [9] S. Biswas, J. Zhang, Z. Li, Y.-Y. Liu, M. Grzywa, L. Sun, D. Volkmer, P. van der Voort, *Dalton Trans.* **2013**, 42, 4730–4737.
- [10] a) Y. Jin, J. Shi, F. Zhang, Y. Zhong, W. Zhu, *J. Mol. Catal. A* **2014**, 383–384, 167–171; b) M. Lin Foo, S. Horike, T. Fukushima, Y. Hijikata, Y. Kubota, M. Takata, S. Kitagawa, *Dalton Trans.* **2012**, 41, 13791–13794.
- [11] a) B. Li, Y. Zhang, D. Ma, L. Li, G. Li, G. Li, Z. Shi, S. Feng, *Chem. Commun.* **2012**, 48, 6151–6153; b) W. J. Phang, H. Jo, W. R. Lee, J. H. Song, K. Yoo, B. Kim, C. S. Hong, *Angew. Chem.* **2015**, DOI: 10.1002/ange.201411703.
- [12] a) T. Ahnfeldt, D. Gunzelmann, J. Wack, J. Senker, N. Stock, *CrystEngComm* **2012**, 14, 4126–4136; b) N. Reimer, B. Gil, B. Marszalek, N. Stock, *CrystEngComm* **2012**, 14, 4119–4125.
- [13] M. Gaab, N. Trukhan, S. Maurer, R. Gummaraju, U. Müller, *Microporous Mesoporous Mater.* **2012**, 157, 131–136.
- [14] A. A. Coelho, Coelho Software, Brisbane, Australia, **2007**.
- [15] G. Socrates, *Infrared and Raman Characteristic Group Frequencies: Tables and Charts*, 3rd ed., Wiley, Hoboken, **2004**.
- [16] J. Canivet, A. Fateeva, Y. Guo, B. Coasne, D. Farrusseng, *Chem. Soc. Rev.* **2014**, 43, 5594–5617.
- [17] M. G. Goesten, J. Juan-Alcañiz, E. V. Ramos-Fernandez, K. B. Sai Sankar Gupta, E. Stavitski, H. van Bekkum, J. Gascon, F. Kapteijn, *J. Catal.* **2011**, 281, 177–187.
- [18] a) E. Alvarez, N. Guillou, C. Martineau, B. Bueken, B. Van de Voorde, C. Le Guillouzer, P. Fabry, F. Nouar, F. Taulelle, D. de Vos, J.-S. Chang, K. H. Cho, N. Ramsahye, T. Devic, M. Daturi, G. Maurin, C. Serre, *Angew. Chem.* **2015**, 127, 3735–3739; b) U. Ravon, G. Chaplais, C. Chizallet, B. Seyyedi, F. Bonino, S. Bordiga, N. Bats, D. Farrusseng, *ChemCatChem* **2010**, 2, 1235–1238.
- [19] a) M. Zhang, Y. Yu, *Ind. Eng. Chem. Res.* **2013**, 52, 9505–9514; b) A. Corma, J. Perez-Pariante, *Clay Miner.* **1987**, 22, 423–433.
- [20] P. F. Siril, H. E. Cross, D. R. Brown, *J. Mol. Catal. A* **2008**, 279, 63–68.
- [21] a) E. Barsoukov, J. R. MacDonald, *Impedance Spectroscopy*, 2nd ed., Wiley, Hoboken, **2005**; b) J. Grehn, J. Krause, *Metzler Physik*, 3rd ed., Schroedel Verlag, Hannover, **1998**.
- [22] G. Alberti, M. Casciola, L. Massinelli, B. Bauer, *J. Membr. Sci.* **2001**, 185, 73–81.

Received: April 17, 2015

Published online on July 17, 2015